Available online at www.sciencedirect.com
SCIENCE DIRECT®
Journal of Sound and Vibration 273 (2004) 125–147
JOURNAL OF SOUND AND VIBRATION
www.elsevier.com/locate/jsvi

Longitudinal vibration analysis of multi-span liquid-filled pipelines with rigid constraints

Ke Yang[a,b], Q.S. Li[b,*], Lixiang Zhang[c]

[a] College of Architectural and Civil Engineering, Wenzhou University, China
[b] Department of Building and Construction, City University of Hong Kong, Tat Chee Avenue, Kowloon, Hong Kong
[c] Department of Mechanics, Kunming University of Science and Technology, China

Received 26 June 2002; accepted 16 April 2003

Abstract

This paper is concerned with vibration analysis considering fluid–structure interaction (FSI) in liquid-filled pipe system using transfer matrix method (TMM) in frequency domain. The emphasis is placing specially upon the multi-span pipe system with middle rigid constraints. Three major mechanisms of coupling, the friction coupling, the Poisson coupling and the junction coupling, as well as both distributed and concentrated external excitations are considered in this study. A phenomenon associated with the rigid constraints, namely, a junction coupling depending on the Poisson coupling and friction coupling (might be called the conditional junction coupling), is revealed and discussed. Numerical examples indicate that the conditional junction coupling has much larger influence on the frequencies of a liquid-filled pipe system than the Poisson coupling does. It is also shown through the numerical examples that the proposed method is efficient.

1. Introduction

The fluid–structure interaction (FSI) in liquid-filled pipe systems has been investigated extensively [1–3]. There are three independent major coupling mechanisms of FSI in pipe systems for longitudinal vibrations. The friction coupling represents a longitudinal interaction caused by friction between fluid and pipe. The Poisson coupling is such an interaction that the change of fluid pressure causes additional hoop stress in pipe wall and then, owing to Poisson ratio, induces corresponding normal stress in pipe wall, and vice versa. The Junction coupling occurs only at the boundaries or the junction of two pipe spans. Mathematically, the Poisson and friction coupling

*Corresponding author. Tel.: +852-2784-4677; fax: +852-2788-7612.
E-mail address: bcqsli@cityu.edu.hk (Q.S. Li).

0022-460X/03/$ - see front matter © 2003 Elsevier Ltd. All rights reserved.
doi:10.1016/S0022-460X(03)00422-X

make the governing equations coupled and cause the equations much different from the traditional ones [4], whereas the junction coupling is usually expressed through the boundary conditions. Among the three coupling mechanisms, the junction coupling is, therefore, the easiest one to deal with.

Thorley [5] was the first who pointed out the existence of precursor waves caused by the Poisson coupling, and Vardy and Fan [6] verified it through a well designed experiment. D'Souza and Oldenburger [7] presented one of the earliest studies in the field. In their paper, the Laplace transform was used to solve an equation including friction and junction coupling. Charley and Caignaert [8] used experimental data to demonstrate that transfer matrices for FSI can predict the measured pressure spectra much better than the classical waterhammer transfer matrices [4], even for simple systems. Charley and Carta [9] presented some recent results on the subject.

Wilkinson [10] presented transfer matrices for the longitudinal, lateral and torsional vibrations of pipes. He studied the junction coupling, but without considering the friction and the Poisson coupling. El-Raheb [11], Nanayakkara and Perreira [12] derived transfer matrices for straight and curved pipes, including the effects of the junction coupling but excluding those of the Poisson and the friction coupling. Kuiken [13] studied the effects of the Poisson and the junction coupling through a numerical simulation. TMM has also been used by Lesmez [14,15], Hatfield [16] et al. and Wiggert et al. [17] (in time domain), Tentarelli and Brown [18] and Brown and Tentarelli [19] (in frequency domain), De Jong [20,21] (in frequency domain). Among them, the friction coupling was considered by Tentarelli and Brown [18] and Brown and Tentarelli [19].

All of the above-mentioned studies did not consider multi-span pipelines with middle constraints. Recently, Wu and Shih [22] developed a TMM for multi-span fluid-conveying pipe. However, they only dealt with the transverse vibration of an Euler–Bernoulli pipe without considering its longitudinal vibration.

Zhang et al. [23] obtained a solution of the four-equation model of FSI in the frequency domain for longitudinal vibration. It has been shown from a series of researches conducted in recent years [24–27] that the frequency-based approaches are efficient for the analysis of FSI in liquid-filled pipe systems. In the present paper, an efficient transfer matrix method for longitudinal vibration analysis of multi-span fluid conveying pipelines with rigid constraints is developed. There are two problems encountered for solving the title problem. Firstly, only variables of fluid can be directly transferred from one span to another, whereas the variables of pipe are usually "separated" by the constraints. The TMM proposed in the present paper can overcome this difficulty by combining the pipe variables into the transfer equations. Secondly, a junction coupling caused by the Poisson coupling, which might be called a conditional junction coupling, may affect the frequency response, which makes the frequencies of liquid in pipes much different from those of the classical case. In the proposed TMM, three major mechanisms of coupling, friction coupling, the Poisson coupling and junction coupling will be considered. In addition to the free vibration analysis, this paper mainly aims at the frequency response analysis of a liquid-filled pipe system. With the proposed TMM, the transient response in time domain would be possibly determined by taking inverse Laplace transform.

In this paper, a pipeline is divided into several spans by rigid constraints (see Fig. 1). A span may consist of several sections. Within a section, the pipe is uniform in geometry and materials. If a concentrated external excitation is acted on a span, we will divide the span into two sections. A node is introduced in the pipe where there is a rigid constraint, or a sudden change in geometry

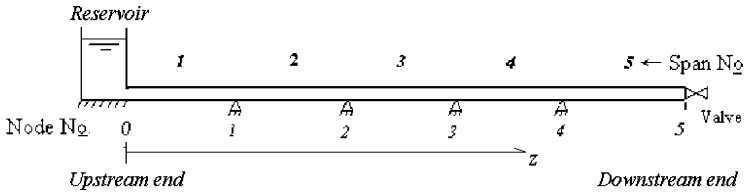

Fig. 1. A multi-span pipe system.

and materials, or a concentrated external excitation is subjected to. The leftmost and rightmost points (see Fig. 1) of the entire pipeline are called the upstream end and downstream end, respectively. At each end, there are two boundary conditions, whereas at a node, there are two compatibility conditions that give a relationship between the variables of the two adjacent pipe sections or spans.

2. The solution for single span pipe system

2.1. The governing equation and its uncoupling

The governing equation for longitudinal vibration of a fluid-filled pipe system can be expressed with matrices as [26]

$$\bar{\mathbf{A}}\frac{\partial \mathbf{y}(z,t)}{\partial t}+\mathbf{B}\frac{\partial \mathbf{y}(z,t)}{\partial z}+\mathbf{C}\mathbf{y}(z,t)=\mathbf{r}(z,t), \tag{1}$$

where $\mathbf{y}(z,t)$ is a vector of unknowns

$$\mathbf{y}(z,t)=[V,H,\dot{u}_z,\sigma_{\mathrm{h}}]^{\mathrm{T}} \tag{2}$$

in which $\dot{u}_z=\dot{u}_z(z,t)$ is the speed along the direction of z, $V=V(z,t)$ is the cross-sectional average speed, $\mathbf{r}(z,t)$ on the right-hand side of Eq. (1) is the external excitation acting along the pipe, $H=H(z,t)$ is the cross-sectional average pressure head of liquid, and $\sigma_{\mathrm{h}}=\sigma_{\mathrm{h}}(z,t)$ is the stress head of pipe wall. $H=H(z,t)$ and $\sigma_{\mathrm{h}}=\sigma_{\mathrm{h}}(z,t)$ are defined below related to pressure $P=P(z,t)$ and normal stress $\bar{\sigma}_z=\bar{\sigma}_z(z,t)$ as

$$H(z,t)=\frac{P(z,t)}{g\rho_{\mathrm{f}}}+z\sin(\gamma)-\frac{P_0(z)}{g\rho_{\mathrm{f}}},\quad \bar{\sigma}_{\mathrm{h}}(z,t)=\frac{\sigma_z(z,t)}{g\rho_{\mathrm{t}}}+z\sin(\gamma)-\frac{\sigma_0(z)}{g\rho_{\mathrm{t}}}, \tag{3}$$

where γ is the elevation angle of the pipe; $P_0(z),\sigma_0(z)$ are the initial pressure and initial stress, respectively; ρ_{t} and ρ_{f} are the density of pipe and liquid, respectively.

Other parameters in Eq. (1) are

$$\bar{\mathbf{A}}=\begin{bmatrix}1 & 0 & 0 & 0\\ 0 & g/c_{\mathrm{F}}^2 & 0 & 0\\ 0 & 0 & 1 & 0\\ 0 & \dfrac{\rho_{\mathrm{f}}gRv}{\rho_{\mathrm{t}}ec_{\mathrm{T}}^2} & 0 & -\dfrac{1}{\rho_{\mathrm{t}}c_{\mathrm{T}}^2}\end{bmatrix},\quad \mathbf{B}=\begin{bmatrix}0 & g & 0 & 0\\ 1 & 0 & -2v & 0\\ 0 & 0 & 0 & -1/\rho_{\mathrm{t}}\\ 0 & 0 & 1 & 0\end{bmatrix} \tag{4}$$

in which

$$c_{\mathrm{F}}^2 = \frac{1}{\rho_{\mathrm{f}}}\left[\frac{1}{K} + \frac{2R(1-v^2)}{eE}\right]^{-1}, \quad c_{\mathrm{T}}^2 = \frac{E}{\rho_{\mathrm{t}}}. \tag{5}$$

In Eq. (5), v is the Poisson ratio, R is the inner radius of pipe, e is the thickness of pipe wall, E is elastic modulus, g is the constant of gravity and K is the bulk modulus of liquid. Matrix $\mathbf{C}$ contains the coefficients of friction and structural viscous damping. When the laminar flow model is adopted, $\mathbf{C}$ is a constant matrix [26].

In Eq. (4), the terms $a_{42} = \rho_{\mathrm{f}} g R v/\rho_{\mathrm{t}} e c_{\mathrm{T}}^2$ and $b_{23} = -2v$ represent the Poisson coupling, which, together with matrix $\mathbf{C}$, make the governing equations coupled.

Taking the Laplace transform, denoted by $L(\cdot)$, for Eq. (1) results in

$$s\mathbf{A}(s)\mathbf{Y}(z,s) + \mathbf{B}\frac{\partial \mathbf{Y}(z,s)}{\partial z} = \bar{\mathbf{r}}(z,s), \tag{6}$$

where

$$\begin{aligned} &\mathbf{Y}(z,s) = L(\mathbf{y}(z,t)),\\ &\mathbf{A}(s) = \bar{\mathbf{A}} + \mathbf{C}/s,\\ &\bar{\mathbf{r}}(z,s) = L(\mathbf{r}(z,t)) + \mathbf{A}(s)\mathbf{y}(z,0) \end{aligned} \tag{7}$$

in which $\mathbf{y}(z,0)$ is a vector of the initial conditions, s is the Laplace variable.

From a generalized eigenvalue problem $|\mathbf{B} - \lambda\mathbf{A}| = 0$, one obtains a diagonal matrix with eigenvalues in the diagonal elements

$$\begin{aligned} \mathbf{\Lambda} &= \mathrm{diag}\{\ \lambda_1(s), \quad \lambda_2(s), \quad \lambda_3(s), \quad \lambda_4(s)\ \}\\ &= \mathrm{diag}\{\ \lambda_1(s), \quad -\lambda_1(s), \quad \lambda_3(s), \quad -\lambda_3(s)\ \}. \end{aligned} \tag{8}$$

Since we deal with a set of hyperbolic partial differential equations, as shown in the second line of Eq. (8), we have $\lambda_2(s) = -\lambda_1(s), \lambda_4(s) = -\lambda_3(s)$. The eigenvalues $\lambda_i(s)$ can be written explicitly [26], and if $\mathbf{C} = 0$, the eigenvalues λ_i, and the elements of the matrices $\mathbf{A}$ and $\mathbf{S}$ are all real numbers independent of s. The full regular matrix $\mathbf{S}(s)$ whose columns are the corresponding eigenvectors is defined from

$$\mathbf{BS}(s) = \mathbf{A}(s)\mathbf{S}(s)\mathbf{\Lambda}(s). \tag{9}$$

Multiplying Eq. (6) with

$$\mathbf{T}(s) = \mathbf{S}^{-1}(s)\mathbf{A}^{-1}(s) \tag{10}$$

and then combined it with Eq. (9), yields

$$s\mathbf{v}(z,s) + \mathbf{\Lambda}\frac{\partial \mathbf{v}(z,s)}{\partial z} = \mathbf{T}(s)\bar{\mathbf{r}}(z,s), \tag{11}$$

where

$$\mathbf{v}(z,s) = \mathbf{T}(s)\mathbf{A}(s)\mathbf{Y}(z,s). \tag{12}$$

Since $\mathbf{\Lambda}$ is a diagonal matrix, Eq. (11) is a set of four independent ordinary equations with complex constant coefficients, and its general solution is

$$\mathbf{v}(z,s) = \mathbf{E}(z,s)\mathbf{v}_0(s) + \mathbf{q}(z,s), \tag{13}$$

where

$$\mathbf{E}(z,s) = \mathrm{diag}\left\{ \exp\left(-\frac{s}{\lambda_1(s)}z\right), \quad \exp\left(\frac{s}{\lambda_1(s)}z\right), \quad \exp\left(-\frac{s}{\lambda_3(s)}z\right), \quad \exp\left(\frac{s}{\lambda_3(s)}z\right) \right\}$$
$$\mathbf{v}(z,s) = \{ v_1, \quad v_2, \quad v_3, \quad v_4 \}^{\mathrm{T}} \quad \mathbf{q}(z,s) = \{ q_1, \quad q_2, \quad q_3, \quad q_4 \}^{\mathrm{T}} \tag{14}$$

$\mathbf{v}_0 = \mathbf{v}_0(s)$ contains undetermined integration constants depending on boundary conditions, and $\mathbf{q}(z,s)$ is a particular solution. When denoting

$$\mathbf{T}\bar{\mathbf{r}} = [\, r_1(z,s), \quad r_2(z,s), \quad r_3(z,s), \quad r_4(z,s) \,]^{\mathrm{T}} \tag{15}$$

the elements of vector $\mathbf{q}(z,s)$ can be determined by

$$q_i = \frac{s\mathrm{e}^{-sz/\lambda_i(s)}}{\lambda_i(s)} \int_0^z r_i(x,s)\mathrm{e}^{-sx/\lambda_i(s)}\,\mathrm{d}x \quad i = 1,2,3,4. \tag{16}$$

From Eqs. (12) and (10), we have

$$\mathbf{Y}(z,s) = \mathbf{K}(z,s)\mathbf{v}_0(s) + \mathbf{Q}(z,s), \tag{17}$$

where regular matrix $\mathbf{K}(z,s)$ and vector $\mathbf{Q}(z,s)$ are defined as

$$\mathbf{K}(z,s) = \mathbf{S}(s)\mathbf{E}(z,s), \quad \mathbf{Q}(z,s) = \mathbf{S}(s)\mathbf{q}(z,s). \tag{18}$$

2.2. The boundary conditions

The original boundary conditions can be found in Ref. [28]. Here we express them in matrix forms, which are convenient for solving the discussed problem. The boundary conditions at an upstream end or downstream end can therefore be

$$[\mathbf{D}(s)]_{2\times 4}\{\mathbf{Y}(\bar{z},s)\}_{4\times 1} = \{\mathbf{f}(s)\}_{2\times 1}, \tag{19}$$

where matrices $\mathbf{D}(s)$ and $\mathbf{f}(s)$ can be determined according to the boundary conditions, and $\bar{z}$ is the co-ordinate of the end (e.g., 0 or the length of the pipe L). The subscripts outside the brackets of Eq. (19) denote the numbers of row and column of the matrix. Thus, for the longitudinal vibration problem, there are two boundary conditions at each end. It will be shown that the boundary conditions involved in the numerical examples of the paper can be written in the form of Eq. (19).

Several boundary conditions are considered here.

- One end with a reservoir, fixed pipe:

$$\mathbf{D}_{\mathrm{r}} = \begin{bmatrix} 0 & 0 & 1 & 0 \\ 0 & 1 & 0 & 0 \end{bmatrix}, \quad \mathbf{f}_{\mathrm{r}}(s) = [\, u_g(s) \quad 0 \,]^{\mathrm{T}} \tag{20}$$

  where u_g denotes the ground velocity, e.g., an earthquake excitation. The constant pressure P_o of the reservoir is taken into account in H (see Eq. (3)). Therefore, if the pipe is horizontally placed, the elevation angle γ is zero, and accordingly at this end $H = 0$.

- Closed valve or closed end with mass m, fixed pipe:

$$\mathbf{D}_R = \begin{bmatrix} 1 & 0 & 0 & 0 \\ 0 & 0 & 1 & 0 \end{bmatrix}, \quad \mathbf{f}_R(s) = [\, u_g(s) \quad u_g(s) \,]^{\mathrm{T}}. \tag{21}$$

- Closed valve or closed end with mass m, longitudinally movable pipe:

$$\mathbf{D}_m = \begin{bmatrix} 1 & 0 & -1 & 0 \\ 0 & g\rho_{\mathrm{f}}A_{\mathrm{f}} & \pm sm & -g\rho_{\mathrm{t}}A_{\mathrm{t}} \end{bmatrix}, \quad \mathbf{f}_m = [\, 0 \quad \pm R_l(s) \,]^{\mathrm{T}}, \tag{22}$$

where $A_{\mathrm{f}}, A_{\mathrm{t}}$ are the area of inner part of the pipe and area of the pipe wall, respectively. m is the mass of the valve or the sealed end. The sign "$\pm$" is determined according to the direction of the co-ordinate and the position where the mass or the excitation appears. R_l is the Laplace transform of the external excitation at the corresponding end.

With the above expressions, the boundary conditions can be expressed in relatively simple and unified forms. For example, when a single span pipe is fixed and connected with a reservoir at the upstream end $z = 0$, and it is fixed and connected with a closed valve at the downstream end $z = L$, then the boundary conditions can be written as

$$\mathbf{D}_{\mathrm{r}}\mathbf{Y}(0, s) = \mathbf{f}_{\mathrm{r}}(s), \quad \mathbf{D}_R\mathbf{Y}(L, s) = \mathbf{f}_R(s). \tag{23}$$

2.3. The frequency domain solution for single span pipe system

For a single and uniform span pipe without middle constraints, assuming that L is the length of the pipe, letting $z = 0$ and $z = L$ in Eq. (16), we get eight relationships between the unknowns and undetermined integration constants

$$\begin{aligned} \mathbf{Y}(0, s) &= \mathbf{K}(0, s)\mathbf{v}_0(s) + \mathbf{Q}(0, s), \\ \mathbf{Y}(L, s) &= \mathbf{K}(L, s)\mathbf{v}_0(s) + \mathbf{Q}(L, s). \end{aligned} \tag{24}$$

At the end $z = 0$ or $z = L$, there are only two boundary conditions:

$$\begin{aligned} \mathbf{D}_{\mathrm{up}}(s)\mathbf{Y}(0, s) &= \mathbf{F}(0, s), \\ \mathbf{D}_{\mathrm{down}}(s)\mathbf{Y}(L, s) &= \mathbf{F}(L, s), \end{aligned} \tag{25}$$

where $\mathbf{D}_{\mathrm{up}}(s), \mathbf{D}_{\mathrm{down}}(s)$ and $\mathbf{F}(0, s), \mathbf{F}(L, s)$ denote the boundary conditions expressed in Eq. (21)–(23) at upstream and downstream end of the pipe, respectively.

Combining Eqs. (23)–(25) yields

$$\begin{aligned} \mathbf{D}_{\mathrm{up}}(s)\mathbf{K}(0, s)\mathbf{v}_0(z, s) &= \mathbf{F}(0, s) - \mathbf{D}_{\mathrm{up}}(s)\mathbf{Q}(0, s), \\ \mathbf{D}_{\mathrm{down}}(s)\mathbf{K}(L, s)\mathbf{v}_0(z, s) &= \mathbf{F}(L, s) - \mathbf{D}_{\mathrm{down}}(s)\mathbf{Q}(L, s). \end{aligned} \tag{26}$$

Eq. (26) can also be written in a matrix form

$$\mathbf{R}(s)\mathbf{v}_0(s) = \bar{\mathbf{F}}(s), \tag{27}$$

where

$$\mathbf{R}(s) = \begin{bmatrix} \mathbf{D}_{\text{up}}\mathbf{K}(0) \\ \mathbf{D}_{\text{down}}\mathbf{K}(L) \end{bmatrix}_{4\times 4}, \tag{28}$$

$$\bar{\mathbf{F}}(s) = \begin{Bmatrix} \mathbf{F}(0) - \mathbf{D}_{\text{up}}\mathbf{Q}(0) \\ \mathbf{F}(L) - \mathbf{D}_{\text{down}}\mathbf{Q}(L) \end{Bmatrix}_{4\times 1}. \tag{29}$$

Eq. (27) is similar to that given in Ref. [26], but it is more concise in form. For a pipe system with more than one pipe sections or spans, Eq. (26) can be applied to different pipe sections, and 0 and L in the equation are the local co-ordinates from upstream node to downstream node.

If the boundary conditions are able to determine all the undetermined constants, $\mathbf{R}$ is certainly regular.

Substituting $\mathbf{v}_0 = \mathbf{R}^{-1}(s)\bar{\mathbf{F}}(s)$ into Eq. (16) one obtains

$$\mathbf{Y}(z,s) = \mathbf{K}(z,s)\mathbf{R}^{-1}(z,s)\bar{\mathbf{F}}(s) + \mathbf{Q}(z,s). \tag{30}$$

3. The transfer matrix method for multi-span pipe systems

A reservoir-pipe-valve (RPV) system with multi-spans is widely used in practices such as in high-pressure pipelines of water power stations. Fig. 1 illustrates a RPV system with N spans numbered $1, 2, \ldots, N$ from upstream to downstream (in Fig. 1, $N = 5$). A point where a rigid constraint located at is called a node, the sequence numbers of nodes are $1, 2, \ldots, N+1$ also from upstream to downstream.

The co-ordinate z (from upstream to downstream) of the ith span is used as local co-ordinate and denoted as z_i. For example, in the ith span, the upstream node, i.e., the $(i-1)$th node, one has $z_i = 0$ and its downstream node, i.e., the $(i+1)$th node, one has a co-ordinate $z_i = L_i$.

3.1. The transfer matrices of the four variables

Recalling that Eq. (17) is hold for all spans, for the ith span it becomes

$$\mathbf{Y}_i(z_i,s) = \mathbf{K}_i(z_i,s)\mathbf{v}_{0i}(s) + \mathbf{Q}_i(z_i,s), \quad i = 1, 2, \ldots, N, \tag{31}$$

where $\mathbf{v}_{0i}(s)$ is a vector of undetermined integration constants related to the ith span (see Eqs. (13) and (14)). Substituting 0 and z_i into Eq. (31), and then eliminating $\mathbf{v}_{0i}(s)$ gives

$$\mathbf{Y}_i(0,s) = \mathbf{F}_i(z_i,s)\mathbf{Y}_i(z_i,s) + \bar{\mathbf{Q}}_i(z_i,s) \tag{32}$$

in which

$$\bar{\mathbf{Q}}_i(z_i,s) = \mathbf{Q}_i(0,s) - \mathbf{F}_i(z_i,s)\mathbf{Q}_i(z_i,s) \tag{33}$$

and the matrix $\mathbf{F}_i$ is called the *field transfer matrix* (for the four variables), defined as

$$\mathbf{F}_i(z_i,s) = \mathbf{K}_i(0,s)\mathbf{K}_i^{-1}(z_i,s) = \mathbf{S}_i(s)\mathbf{E}^{-1}(z_i,s)\mathbf{S}_i^{-1}(s). \tag{34}$$

We can also write $\mathbf{F}_i$ in the following form

$$\mathbf{F}_i = \begin{bmatrix} \mathbf{F}_{(i)11} & \mathbf{F}_{(i)12} \\ \mathbf{F}_{(i)21} & \mathbf{F}_{(i)22} \end{bmatrix}. \tag{35}$$

From Eq. (34), it can be seen that the diagonal sub-matrices $\mathbf{F}_{(i)11}$ and $\mathbf{F}_{(i)22}$ of $\mathbf{F}_i$ corresponding to the non-FSI motions of fluid and pipe, respectively. The non-diagonal sub-matrices $\mathbf{F}_{(i)12}$ and $\mathbf{F}_{(i)21}$ represent the Poisson coupling and the friction coupling, respectively. For example, if $\mathbf{C} = 0$, the matrices $\mathbf{S}$ and $\mathbf{S}^{-1}$can be written explicitly in the form [27]

$$\mathbf{S}_{(i)} = \begin{bmatrix} \mathbf{S}_{11} & v\mathbf{S}_{12} \\ v\mathbf{S}_{21} & \mathbf{S}_{22} \end{bmatrix}_{(i)}, \quad \mathbf{S}_{(i)}^{-1} = \begin{bmatrix} \mathbf{s}_{11} & v\mathbf{s}_{12} \\ v\mathbf{s}_{21} & \mathbf{s}_{22} \end{bmatrix}_{(i)}, \tag{36}$$

where all the sub-matrices $\mathbf{S}_{ij}$ and $\mathbf{s}_{ij}$ $(i,j = 1,2)$ are finite and non-zero. From Eq. (34), it is easy to know that the non-diagonal sub-matrices $v\mathbf{F}_{12}$ and $v\mathbf{F}_{21}$ of $\mathbf{F}$ must also be of the form like the non-diagonal sub-matrices of $\mathbf{S}$ or $\mathbf{S}^{-1}$. Thus, when $v = 0$, $\mathbf{F}_{(i)12}$ and $\mathbf{F}_{(i)21}$ of $\mathbf{F}_i$ are equal to zero. Eq. (32) is then uncoupled, and becomes two sets of independent equations, each represents the motion of fluid or pipe.

We consider, at first, a span consisting of M sections (with $M-1$ middle sub-nodes) with different cross-sections, materials and thickness of the pipe wall and so on. It is assumed $\bar{\mathbf{Q}}_i(z_i, s) = 0$, indicating that there is no external force (see Eq. (16)) acting on the system. Evidently, Eq. (34) can also be applied to each of such sections, on condition that z_i is adopted as the local co-ordinate within the section. Thus, the compatibility conditions at a node between two sections are

$$\mathbf{D}_j\mathbf{Y}_j(L_j, s) = \mathbf{D}_{j+1}\mathbf{Y}_{j+1}(0, s) \quad j = 1, 2, \ldots, M, \tag{37}$$

where

$$\mathbf{D}_j = \begin{bmatrix} A_{\mathrm{f}(j)} & 0 & -A_{\mathrm{f}(j)} & 0 \\ 0 & 1 & 0 & 0 \\ 0 & 0 & 1 & 0 \\ 0 & A_{\mathrm{f}(j)} & 0 & A_{\mathrm{t}(j)} \end{bmatrix}$$

in which $A_{\mathrm{f}(j)}$ and $A_{\mathrm{t}(j)}$ are the area of liquid and the pipe wall in the ith section, respectively. Obviously, the matrix $\mathbf{D}_j$ is regular. Thus the relationship between the variables of the upstream and downstream sides of a node is then

$$\mathbf{Y}_j(L_j, s) = \mathbf{P}_j\mathbf{Y}_{j+1}(0, s) \tag{38}$$

in which the matrix

$$\mathbf{P}_j = \mathbf{D}_j^{-1}\mathbf{D}_{j+1} \tag{39}$$

is the *point transfer matrix* (for the four variables).

The point transfer matrix $\mathbf{P}_j$ in Eq. (39) and the field transfer matrix $\mathbf{F}_i$ (with subscript j) in Eq. (34) can be used to obtain the transfer matrix for a span with several sections easily. For examples, the global transfer matrix may be (see Fig. 1 and assuming that there is no rigid constraint)

$$\mathbf{N} = \mathbf{F}_1\mathbf{P}_1\mathbf{F}_2\mathbf{P}_2, \ldots, \mathbf{F}_i\mathbf{P}_i, \ldots, \mathbf{F}_{M-1}\mathbf{P}_{M-1}. \tag{40}$$

With the global transfer matrix **N**, the relationship between the variables of both upstream end and downstream end of such a span is

$$\mathbf{Y}_1(0,s) = \mathbf{N}\mathbf{Y}_M(0,s) = \mathbf{N}\mathbf{F}_M\mathbf{Y}_M(L_M,s). \tag{41}$$

In some sense, Eq. (41) condense all sections in a span into a single uniform section.

3.2. The field transfer matrix of fluid variables

Assuming that the local loss of energy at a rigid constraint is neglected, the compatibility conditions at the ith rigid constraint, which connects the ith and $(i+1)$th spans, are

$$\text{Equal discharge}: \quad V_{\mathrm{U}(i+1)}A_{\mathrm{f}(i+1)} = V_{\mathrm{D}(i)}A_{\mathrm{f}(i)}, \tag{42}$$

$$\text{Equal pressure}: \quad H_{\mathrm{U}} = H_{\mathrm{D}}, \tag{43}$$

$$\text{Zero displacement}: \quad \dot{u}_{\mathrm{U}(i+1)} = 0, \quad \dot{u}_{\mathrm{D}(i)} = 0, \tag{44}$$

where, the variables at upstream node and downstream node of a span are identified with subscripts U and D, respectively. In the compatibility conditions (Eqs. (42)–(44)), the stresses at both spans do not appear, which makes it impossible to establish the point transfer matrix and to get a relationship shown in Eq. (37).

In order to perform the transfer, denoting

$$\mathbf{x}(z,s) = L\begin{Bmatrix} V(z,t) \\ H(z,t) \end{Bmatrix}, \tag{45}$$

$$U(z,s) = L(\dot{u}(z,t)), \tag{46}$$

$$\sigma(z,s) = L(\sigma_{\mathrm{h}}(z,t)) \tag{47}$$

thus, one obtains

$$\mathbf{Y}(z,s) = \begin{Bmatrix} \mathbf{x}(z,s) \\ U(z,s) \\ \sigma(z,s) \end{Bmatrix}. \tag{48}$$

For the ith span, the unknowns are identified with subscript i as $\mathbf{x}_{(i)}(z,s)$, $U_{(i)}(z,s)$, $\sigma_{(i)}(z,s)$.

The transform matrix of the ith span can be rewritten as

$$\mathbf{F}_{(i)} = \mathbf{F}_{(i)}(L_i,s) = \left[\begin{array}{cc|cc} F_{(i)11} & F_{(i)12} & F_{(i)13} & F_{(i)14} \\ F_{(i)21} & F_{(i)22} & F_{(i)23} & F_{(i)24} \\ \hline F_{(i)31} & F_{(i)32} & F_{(i)33} & F_{(i)34} \\ F_{(i)41} & F_{(i)42} & F_{(i)43} & F_{(i)44} \end{array}\right]. \tag{49}$$

With the above-introduced expressions, Eq. (32), taking $z_i = L_i$, becomes

$$\begin{Bmatrix} \mathbf{x}_{(i)}(0,s) \\ U_{(i)}(0,s) \\ \sigma_{(i)}(0,s) \end{Bmatrix} = \begin{bmatrix} \mathbf{F}_{(i)11} & \mathbf{F}_{(i)12} \\ \mathbf{F}_{(i)21} & \mathbf{F}_{(i)22} \end{bmatrix} \begin{Bmatrix} \mathbf{x}_{(i)}(L_i,s) \\ U_{(i)}(L_i,s) \\ \sigma_{(i)}(L_i,s) \end{Bmatrix} + \bar{\mathbf{Q}}_i(s). \tag{50}$$

If the up- and downstream nodes of the ith span are both rigid constrained, we have

$$U_{(i)}(0,s) = 0 \quad \text{and} \quad U_{(i)}(L_i,s) = 0. \tag{51}$$

Substituting Eq. (51) into Eq. (50) yields

$$\sigma_{(i)}(L_i,s) = -\left(\frac{1}{F_{(i)34}}[\,F_{(i)31} \quad F_{(i)32}\,]\mathbf{x}_{(i)}(L_i,s) - \bar{Q}_{(i)3}\right), \tag{52}$$

where $\bar{Q}_{(i)3}$ is the third row of the vector $\bar{\mathbf{Q}}_i(s)$. As shown in Fig. 1, only node No. 5 may not satisfy this condition.

Thus, the variables of the pipe in this span are either zero (for velocity) or can be expressed with the fluid variables $\mathbf{x}_{(i)}$ (for stress in pipe wall). This implies that only fluid variables need transferring.

The first two rows of Eq. (50) give

$$\mathbf{x}_{(i)}(0,s) = \mathbf{F}_{(i)11}\mathbf{x}_{(i)}(L_i,s) + \begin{Bmatrix} F_{(i)14} \\ F_{(i)24} \end{Bmatrix}\sigma_{(i)}(L_i,s) + \begin{Bmatrix} \bar{Q}_{(i)1} \\ \bar{Q}_{(i)2} \end{Bmatrix} \tag{53}$$

substituting Eq. (52) into Eq. (53) leads to

$$\mathbf{x}_{(i)}(0,s) = \mathbf{F}_{x(i)}\mathbf{x}_{(i)}(L_i,s) + \bar{\mathbf{Q}}_{x(i)}, \quad i = 2,3,\ldots,N-1, \tag{54}$$

where

$$\bar{\mathbf{Q}}_{x(i)} = \begin{Bmatrix} \bar{Q}_{(i)1} \\ \bar{Q}_{(i)2} \end{Bmatrix} + \frac{1}{F_{(i)34}}\begin{Bmatrix} F_{(i)14} \\ F_{(i)24} \end{Bmatrix}\bar{Q}_{(i)3} \tag{55}$$

$\mathbf{F}_{x(i)}$ in Eq. (54) is called *the transfer matrix for fluid* in the ith span and is defined as

$$\mathbf{F}_{x(i)} \equiv \frac{1}{F_{(i)34}}\begin{bmatrix} F_{(i)34}F_{(i)11} - F_{(i)14}F_{(i)31} & F_{(i)34}F_{(i)12} - F_{(i)14}F_{(i)32} \\ F_{(i)34}F_{(i)21} - F_{(i)24}F_{(i)31} & F_{(i)34}F_{(i)22} - F_{(i)24}F_{(i)32} \end{bmatrix}. \tag{56}$$

Considering that the upstream end may have other kinds of boundary conditions different from those shown in Fig. 1, Eq. (54) may not be valid for the first span, although both sides are rigid constrained. Therefore, in Eq. (54), the span number i begins from 2 rather than 1.

It is obvious that the first term in Eq. (53) is related to fluid only. However, it contains the effect of the Poisson coupling (see Eqs. (34) and (36)). If $v = 0$, it will become the same case as what we can obtain from the classical waterhammer theory [4]. The second term in Eq. (53) represents the influence of pipe on fluid owing to all of the three kinds of coupling. As a matter of fact, when the Poisson coupling and friction coupling are neglected, the middle constraints will make no influence on the fluid (see Eq. (1)). As in the case of $\mathbf{C} = 0$, if the Poisson ratio of pipe wall is equal to zero, the second term of Eq. (53) will become zero because of the disappearance of $\mathbf{F}_{(i)12}$ and

$\mathbf{F}_{(i)21}$ in Eq. (35). Therefore, the second term of Eq. (53) corresponds to the junction coupling related to the Poisson coupling and friction coupling. Although caused by compatibility conditions at a node, it is somewhat different from junction coupling, since its existence depends upon the other two kinds of coupling. For this reason, it might be called conditional junction coupling. We will illustrate this phenomenon later. In fact, it has much larger influence on the frequencies of a pipe system than the Poisson coupling does (by comparing Fig. 3(a) with Fig. 6(a)).

3.3. The point and global transfer matrix of fluid variables

Taking the Laplace transform to the constrained conditions, Eqs. (42) and (43), and expressed with matrix $\mathbf{x}_{(i)}$ gives

$$\mathbf{x}_{(i)}(L_i, s) = \mathbf{P}_{x(i)}\mathbf{x}_{(i+1)}(0, s), \quad i = 1, 2, \ldots, N-1, \tag{57}$$

where $\mathbf{P}_{x(i)}$ is the *point transfer matrix for fluid* defined by

$$\mathbf{P}_{x(i)} = \begin{bmatrix} A_{\mathrm{f}(i+1)}/A_{\mathrm{f}(i)} & 0 \\ 0 & 1 \end{bmatrix}. \tag{58}$$

Obviously, $\mathbf{P}_{x(i)}$ is different from the point transfer matrix $\mathbf{P}_i$ defined in Eq. (39).

With the field transfer matrix $\mathbf{F}_{x(i)} = \mathbf{F}_{x(i)}(L_i, s)$ in Eq. (54) (taking $z_i = L_i$) and the point transfer matrix $\mathbf{P}_{x(i)}$ in Eq. (57), the relationship between the upstream fluid variables of the ith constrained span and the upstream fluid variables of the $(i+1)$th constrained span is found to be

$$\mathbf{x}_{(i)}(0, s) = \mathbf{F}_{x(i)}\mathbf{x}_{(i)}(L_i, s) + \bar{\mathbf{Q}}_{x(i)}, \quad i = 1, 2, \cdots, N-1, \tag{59}$$

$$\mathbf{x}_{(i)}(0, s) = \mathbf{F}_{x(i)}\mathbf{P}_{x(i)}\mathbf{x}_{(i+1)}(0, s) + \bar{\mathbf{Q}}_{x(i)}, \quad i = 1, 2, \cdots, N-1. \tag{60}$$

Combining Eqs. (59) and (60) yields

$$\mathbf{x}_{(2)}(0, s) = \mathbf{N}_{x(N-1)}\mathbf{x}_{(N)}(0, s) + \sum_{i=1}^{N-2}(\mathbf{N}_{x(i)}\bar{\mathbf{Q}}_{x(i+1)}), \tag{61}$$

where $\mathbf{N}_{x(i)}$ is the global transfer matrix

$$\mathbf{N}_{x(i)} = \begin{cases} \prod_{j=2}^{i}\mathbf{F}_{x(j)}\mathbf{P}_{x(j)} & 2 < i \leqslant N-1, \\ \mathbf{I} & i = 1. \end{cases} \tag{62}$$

Therefore, for all constrained spans, we have

$$\mathbf{x}_{(1)}(L_1, s) = \mathbf{P}_{x(1)}\mathbf{x}_{(2)}(0, s) = \mathbf{P}_{x(1)}\mathbf{N}_{x(N-1)}\mathbf{x}_{(N)}(0, s) + \mathbf{P}_{x(1)}\sum_{j=1}^{N-2}(\mathbf{N}_{x(j)}\bar{\mathbf{Q}}_{x(j+1)}). \tag{63}$$

As for the case shown in Fig. 1, the above equation becomes

$$\begin{aligned}\mathbf{x}_{(1)}(L_1, s) = {} & \mathbf{P}_{x(1)}\mathbf{F}_{x(2)}\mathbf{P}_{x(2)}\mathbf{F}_{x(3)}\mathbf{P}_{x(3)}\mathbf{F}_{x(4)}\mathbf{P}_{x(4)}\mathbf{x}_{(5)}(0, s) \\ & + \mathbf{P}_{x(1)}(\mathbf{F}_{x(2)}\mathbf{P}_{x(2)}\mathbf{F}_{x(3)}\mathbf{P}_{x(3)}\bar{\mathbf{Q}}_{x(4)} + \mathbf{F}_{x(2)}\mathbf{P}_{x(2)}\bar{\mathbf{Q}}_{x(3)} + \bar{\mathbf{Q}}_{x(2)}),\end{aligned} \tag{64}$$

Eq. (64) establishes the relationship between the downstream fluid variables of the first span $\mathbf{x}_{x(1)}(L_1, s)$ and the upstream fluid variables of the last span $\mathbf{x}_{(5)}(0, s)$. It is noted that Eq. (64) is not

a relationship between variables of nodes 1 and 5, as normally at the two nodes the pipe is not necessarily rigid constrained.

For a multi-span pipeline, Eq. (63) play a similar role as Eq. (57) for a two span pipeline. Eq. (63) condenses all nodes of a constrained span into a single node, just like Eq. (41) condenses all sections into a single uniform section.

3.4. The final equation and its solution

By using the field transfer matrix in Eq. (32) for the first and the last spans, we have

$$\mathbf{Y}_1(0,s) = \mathbf{F}_1\mathbf{Y}_1(L_1,s) + \bar{\mathbf{Q}}_1(s), \tag{65}$$

$$\mathbf{Y}_N(0,s) = \mathbf{F}_N\mathbf{Y}_N(L_N,s) + \bar{\mathbf{Q}}_N(s) \tag{66}$$

and the boundary conditions at upstream end and downstream end leads to

$$\mathbf{D}_\mathrm{U}\mathbf{Y}_1(0,s) = \bar{\mathbf{F}}_\mathrm{U}, \tag{67}$$

$$\mathbf{D}_\mathrm{D}\mathbf{Y}_N(L_N,s) = \bar{\mathbf{F}}_\mathrm{D}. \tag{68}$$

Combining Eqs. (65) and (67) yields

$$\mathbf{D}_\mathrm{U}\mathbf{F}_1\mathbf{Y}_1(L_1,s) = \bar{\mathbf{F}}_\mathrm{U} - \mathbf{D}_\mathrm{U}\bar{\mathbf{Q}}_1(s). \tag{69}$$

Combining Eqs. (66) and (68) yields

$$\mathbf{D}_\mathrm{D}\mathbf{F}_N^{-1}\mathbf{Y}_N(0,s) = \bar{\mathbf{F}}_\mathrm{D} + \mathbf{D}_\mathrm{D}\mathbf{F}_N^{-1}\bar{\mathbf{Q}}_N(s). \tag{70}$$

The compatibility conditions of the first and the last rigid constraints give

$$U_1 = 0, \quad U_{N-1} = 0. \tag{71}$$

Eqs. (69)–(71) and (63) are 8 equations including 8 variables that are required to solve. They can be written in matrix form as

$$\begin{bmatrix} \mathbf{D}_\mathrm{U}\mathbf{F}_1 & \mathbf{0}_{2\times4} \\ \mathbf{0}_{2\times4} & \mathbf{D}_\mathrm{D}\mathbf{F}_N^{-1} \\ \mathbf{I}_\mathrm{U} & \mathbf{I}_\mathrm{D} \\ \mathbf{I}_0 & \bar{\mathbf{N}}_{N-1} \end{bmatrix}_{8\times8} \begin{Bmatrix} \mathbf{Y}_1(L_1,s \\ \mathbf{Y}_N(0,s) \end{Bmatrix} = \begin{Bmatrix} \bar{\mathbf{F}}_\mathrm{U} - \mathbf{D}_\mathrm{U}\bar{\mathbf{Q}}_1(s) \\ \bar{\mathbf{F}}_\mathrm{D} + \mathbf{D}_\mathrm{D}\mathbf{F}_N^{-1}\bar{\mathbf{Q}}_N(s) \\ \mathbf{0}_{2\times1} \\ \mathbf{P}_{x(1)}\sum_{j=0}^{N-2}(\mathbf{N}_{x(j)}\bar{\mathbf{Q}}_{x(j+1)}) \end{Bmatrix}_{8\times1} \tag{72}$$

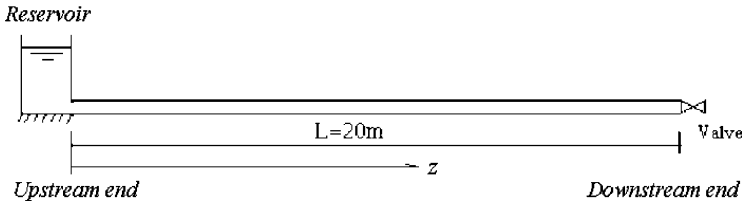

Fig. 2. A single span RPV system.

Table 1
Geometrical and material properties of the RPV system

Steel pipe	Water
$L = 20$ m length	$K = 2.1$ GPa, bulk modulus
$R = 398.5$ mm inner radius	$\rho_t = 1000\,\mathrm{kg/m^3}$ density
$e = 8$ mm pipe wall thickness	
$E = 210$ GPa Young's modulus	
$v = 0.3$ Poisson ratio	
$\rho_t = 7900\,\mathrm{kg/m^3}$ density of pipe	

Table 2
Frequencies of the single span pipe with different Poisson ratios and two boundary conditions

Mode	Valve is free					Valve is constrained			
	Ref. [26] $v = 0.3$	$v = 0.0$	$v = 0.1$	$v = 0.2$	$v = 0.3$	$v = 0.0$	$v = 0.1$	$v = 0.2$	$v = 0.3$
1	12	11.4	11.7	12.0	12.4	12.8	12.8	12.9	13.1
2	32	33.6	33.0	32.4	31.8	38.5	38.5	38.5	38.5
3	56	54.4	54.8	55.2	55.7	64.1	64.1	64.1	64.0
4	73	73.9	73.6	73.4	73.2	89.7	89.7	89.7	89.6
5	97	94.7	95.3	96.1	96.9	115.4	115.3	115.2	115.1
6	116	116.9	116.6	116.4	116.2	128.9	129.3	130.3	131.8
7	141	139.7	140.0	140.5	141.0	141.0	141.0	141.1	141.3
8	161	161.9	161.4	160.9	160.5	166.7	166.7	166.6	166.6
9	185	182.8	183.2	183.8	184.5	192.3	192.3	192.2	192.1

in which

$$\mathbf{I}_U = \begin{bmatrix} 0 & 0 & 1 & 0 \\ 0 & 0 & 0 & 0 \end{bmatrix}, \quad \mathbf{I}_D = \begin{bmatrix} 0 & 0 & 0 & 0 \\ 0 & 0 & 1 & 0 \end{bmatrix}, \tag{73}$$

$$\mathbf{I}_o = \begin{bmatrix} 1 & 0 & 0 & 0 \\ 0 & 1 & 0 & 0 \end{bmatrix}, \quad \tilde{\mathbf{N}}_{N-1} = [\,-\mathbf{P}_{x(1)}\mathbf{N}_{x(N-1)} \quad \mathbf{0}_{2\times 2}\,]. \tag{74}$$

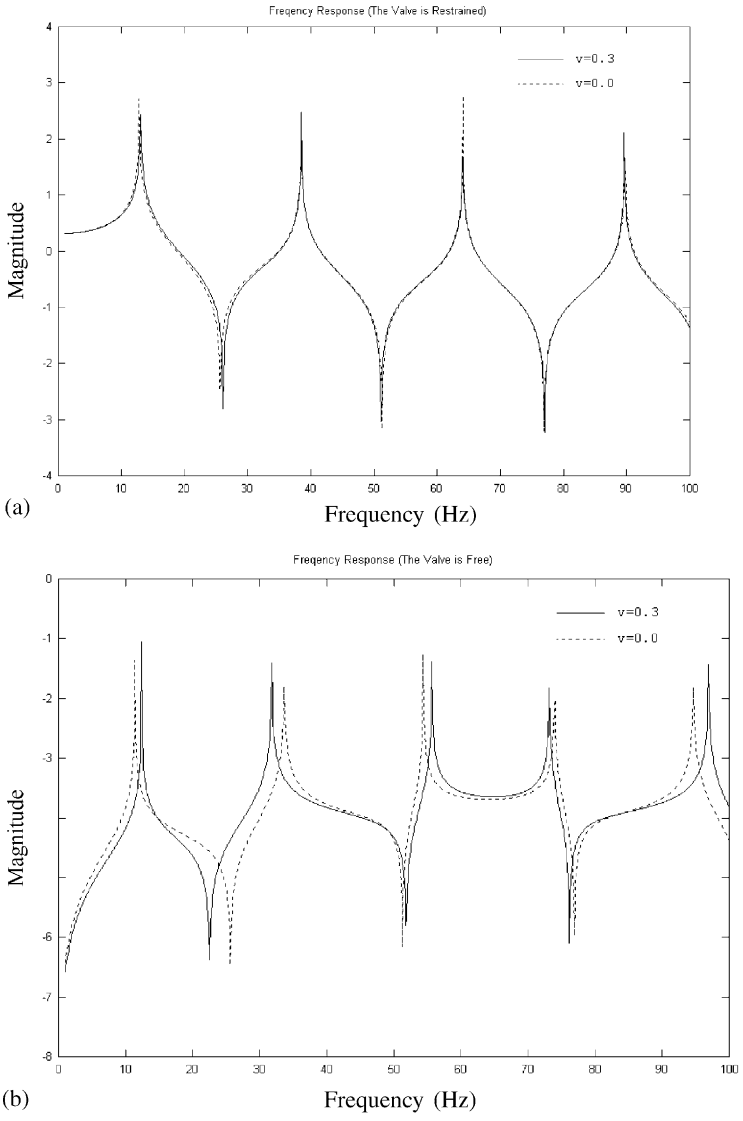

Fig. 3. Frequency response of the single span pipe. (a) Valve is rigid constrained, (b) valve is free.

After obtaining the above 8 variables at the downstream end of the first and the upstream end of the last span, we can calculate the frequency responses at any point z_i of the constrained spans, by using Eqs. (57), (54), (48) and (32).

4. Numerical examples

Two cases of a RPV system are considered in the examples. Case 1: the valve is rigid constrained. Case 2: the valve is free. Also in all the examples of this paper, the valve is assumed to

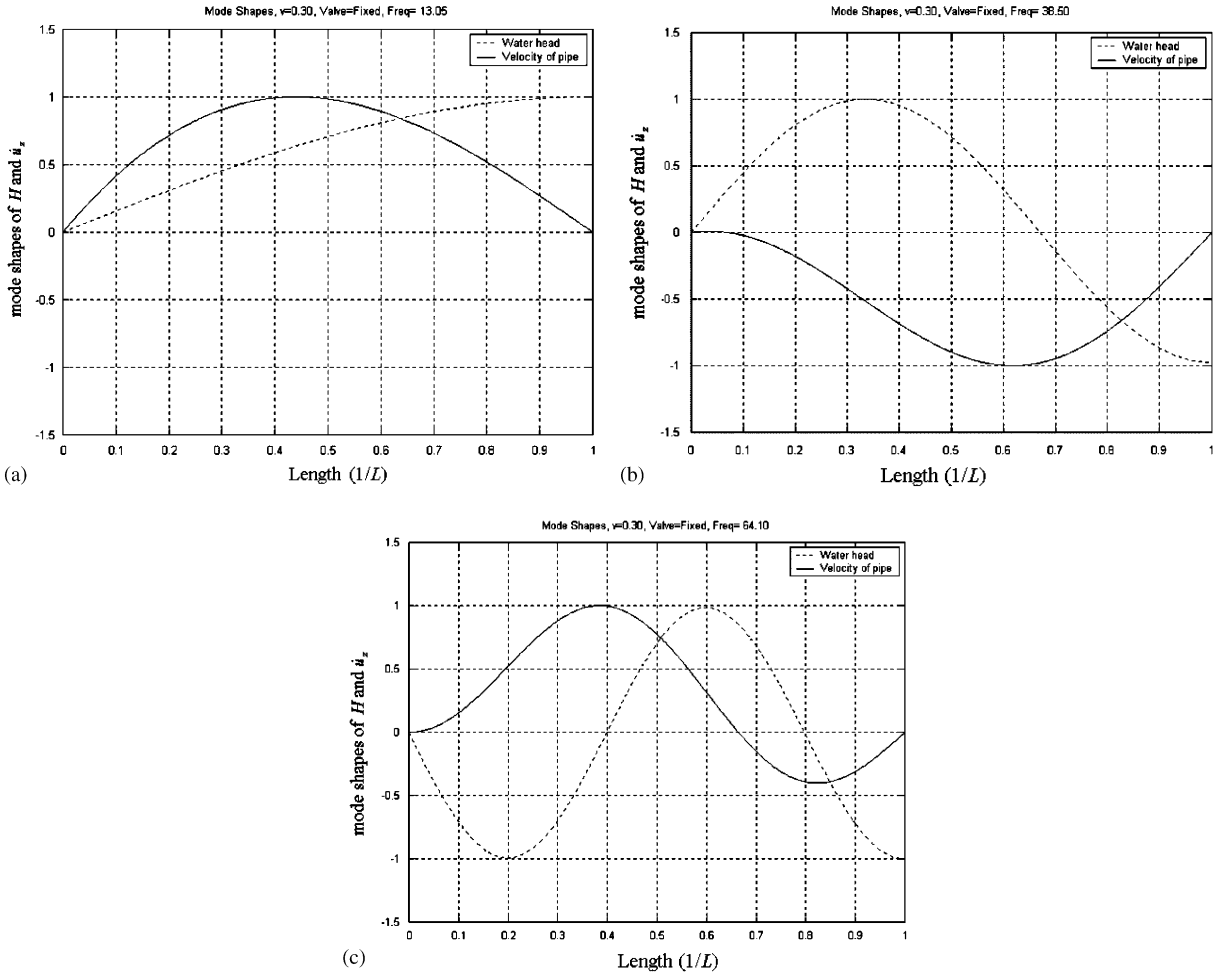

Fig. 4. Modes 1–3 of the single span pipe with constrained valve.

be instantaneously closed, and the mass m of the valve in Eq. (22) is assumed to be zero. For the friction matrix in Eq. (1), we have $\mathbf{C} = 0$.

4.1. Single span pipeline with 20 m in length

First of all, a system with single span, as shown in Fig. 2, is considered here for comparison purposes. The parameters of the system are listed in Table 1, which are the same as those used by Zhang et al. [26].

The predicted frequencies are listed in Table 2 together with the results of Case 2 obtained by Zhang et al. [26].

It is shown in Table 2 and Fig. 3 that for Case 2, the liquid-pipe coupling (including the Poisson coupling and the junction coupling) influences the frequencies significantly. For Case 1, the difference of frequencies is rather small mainly due to no existence of junction coupling and to the large stiffness of the pipe wall.

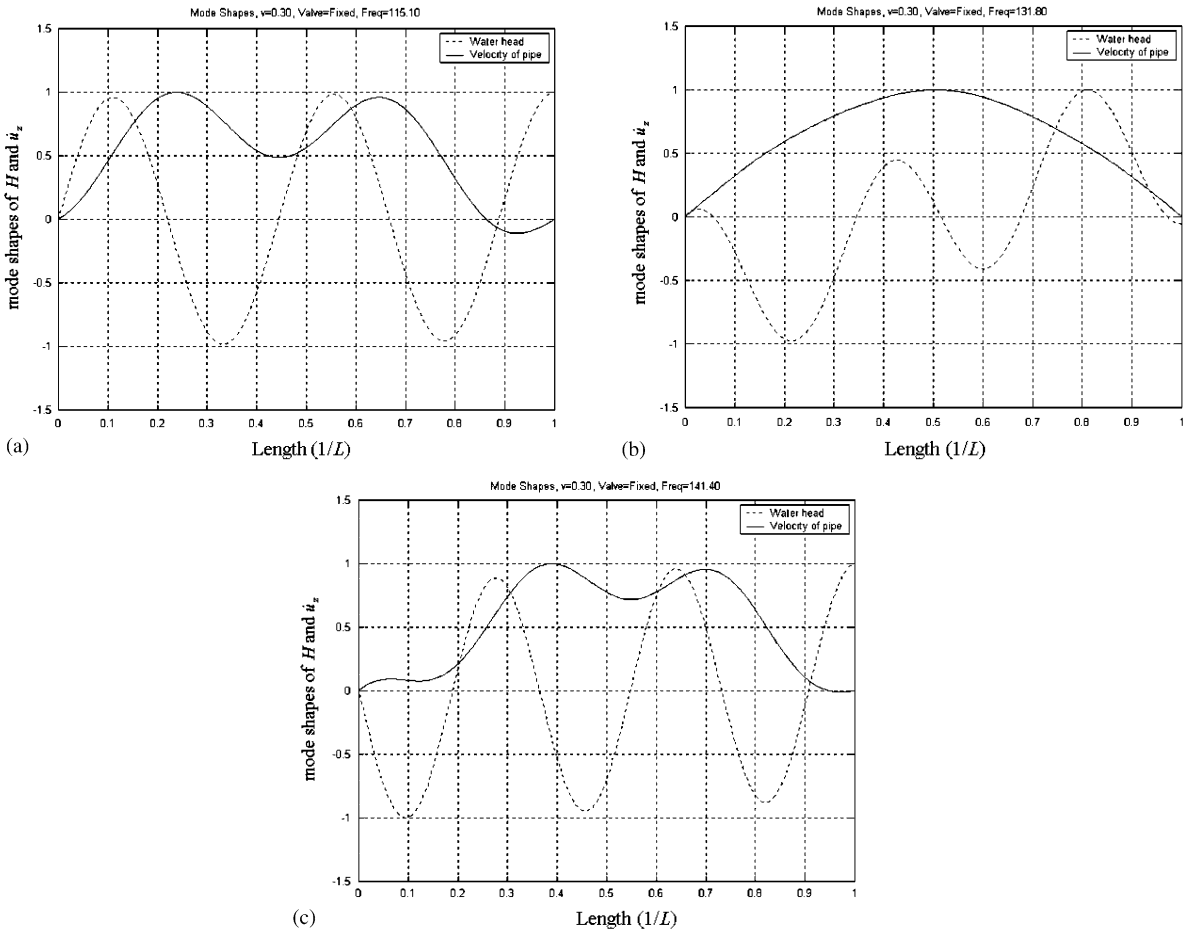

Fig. 5. The 1st pipe mode shapes of and two nearby fluid mode shapes of the single span pipe with constrained valve. (a) Mode shape 5th (fluid), (b) mode shape 6th (pipe), (c) mode shape 7th (fluid).

Theoretically, all the modes belong to the system, since the FSI makes the modes interacting (or coupling) each other. On the other hand, when without FSI, the modes will separate into independent modes of fluid and modes of pipe, respectively. Although in case with FSI, we can only say the mode of the system. However, we can tell which comes from the separated fluid mode and which originates from the separated pipe mode. Thus, the pipe mode and the fluid mode are mentioned below, although they are not absolutely independent. To illustrate this, considering Fig. 4 first, which shows the first three mode shapes of a single span pipe for Case 1. The three modes mainly belong to the fluid; the vibration of the pipe is caused by the fluid through coupling. As a result, for example, the mode of the velocity of the pipe, as shown in Fig. 5(a), is not symmetry. Fig. 5(b) shows the 6th mode shape of the system (the first mode shape of the pipe), which is symmetry. Evidently, in this mode, the pipe induces the vibration of the liquid. In contrast with this observation, the 5th and 7th mode shapes of the system (mode shape of fluid, as shown inFig. 5(a) and (b)) suggest that the fluid vibrates with their own mode shapes. Liquid

Table 3
Frequencies of the multi-span pipe system with different lengths

Mode	Pipeline length = 5 * 4 m				Pipeline length = 5 * 20 m			
	$v = 0.0$		$v = 0.3$		$v = 0.0$		$v = 0.3$	
	Restrained valve	Free valve	Restrained valve	Free valve	Restrained valve	Free valve	Restrained valve	Free valve
1	12.8	12.5	13.1	13.1	2.6	2.5	2.6	2.6
2	38.5	37.5	39.3	39.0	7.7	7.5	7.9	7.8
3	64.1	62.5	65.3	64.6	12.8	12.5	13.1	12.9
4	89.7	87.5	91.1	89.3	17.9	17.5	18.2	17.9
5	115.4	112.4	116.6	112.8	23.1	22.5	23.3	22.6
6	141.0	137.3	142.1	137.1	28.2	27.5	28.4	27.4
7	166.7	162.1	167.2	160.5	33.3	32.4	33.4	32.1
8	192.3	186.8	192.4	185.1	38.5	37.4	38.5	37.0
9	218.0	211.4	217.7	210.4	43.6	42.3	43.5	42.1

induces the pipe's vibration, in which the curves have two or three peaks as the same number of peaks as those in the curves of the water head.

4.2. Multi-span pipeline with 20 m in length

To illustrate the application of the present transfer matrix method, a RPV system (see Fig. 1.) is used as an example. Like the single span pipe system shown in Fig. 2, all the parameters in Table 1 remain unchanged for this example. However, the pipeline considered in this example is divided into 5 equal spans with 4 m in length for each span (the total length of the pipe remains 20 m).

In Case 1, because the valve is also rigid constrained, all the boundary conditions and compatibility conditions may cause junction coupling. Therefore, if the Poisson ratio is equal to zero, the frequencies of the system are, as expected, the same as those of a single span pipe (see column 2 of Table 3 and column 7 of Table 2). This implies that the constraints do not have any effect on the frequencies of fluid, when there is no liquid-pipe coupling.

On the other hand, in Case 2 (the valve is free), the junction coupling takes place at the downstream end (at the valve). The shorting of the last pipe span results in the increase of the frequencies (see column 3 of Table 3 and column 3 of Table 2).

When comparing Fig. 6(a) with Fig. 3(a), we will find that when the same pipe is rigidly constrained in 4 middle nodes, the differences of the frequencies between $v = 0.3$ and $v = 0.0$ are large. In Fig. 3(a) the little differences of the frequencies for each mode between $v = 0.3$ and $v = 0.0$ is found owing to the Poisson coupling only. However, in Fig. 6(a), larger differences exist because of the Poisson coupling and mainly due to the so called conditional junction coupling.

4.3. Multi-span pipeline with 20 m in length for each span

In this example, we consider a pipeline, with 5 spans and 20 m in length for each span, 100 m length in total. Other parameters in Table 1 remain unchanged for this example. The predicted

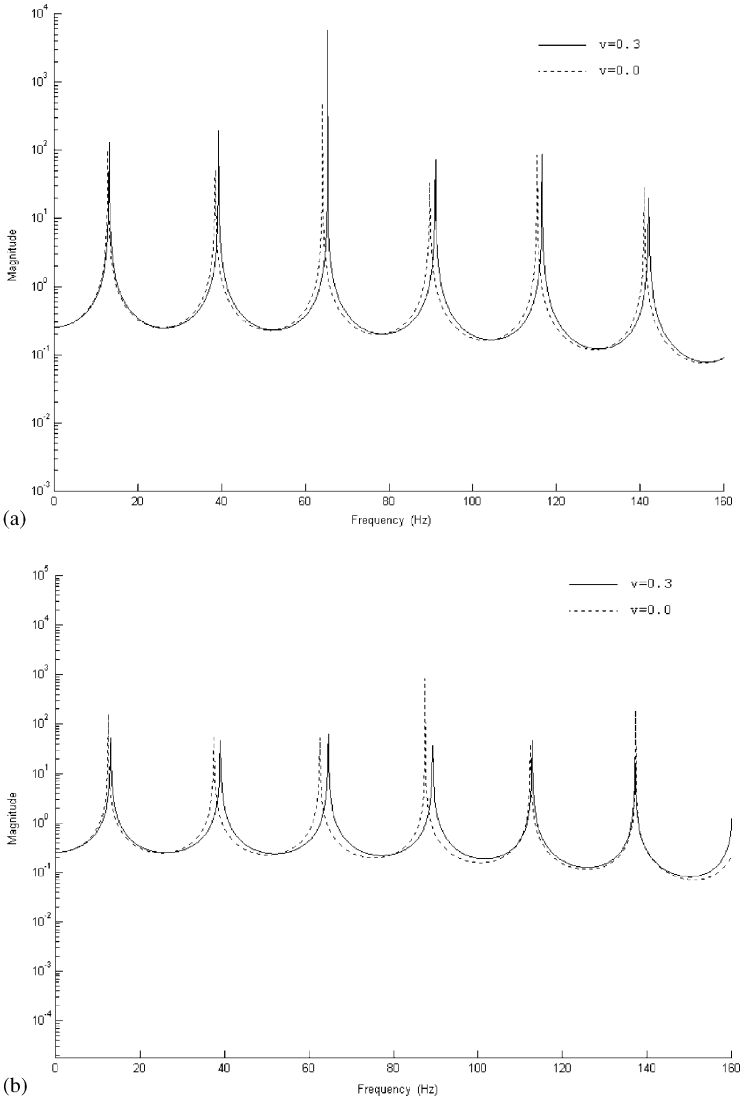

Fig. 6. Frequency responses of the RPV system with 5 spans (4 m length for each span). (a) Valve is rigid constrained, (b) valve is free.

frequencies (with or without the Poisson coupling, Case 1 and Case 2) are listed in columns 6–9 of Table 3. The corresponding frequency responses are illustrated in Fig. 7(a) and (b). As the total length of the pipeline is enlarged by 5 times, the frequencies of fluid are about 1/5 of those of a single span pipeline accordingly.

Fig. 8 shows the first three mode shapes of the system for Case 1. In the Figure, the rigid constraints are placed at 0, 0.2, 0.4, 0.6,0.8 and $1.0/L$ where the velocity of the pipe is zero. The first three mode shapes are mainly caused by the fluid. The first mode shape of the pipe (the 32nd mode of the system) is shown in Fig. 9(a). By comparing Fig. 9(a) with a nearby fluid mode shape

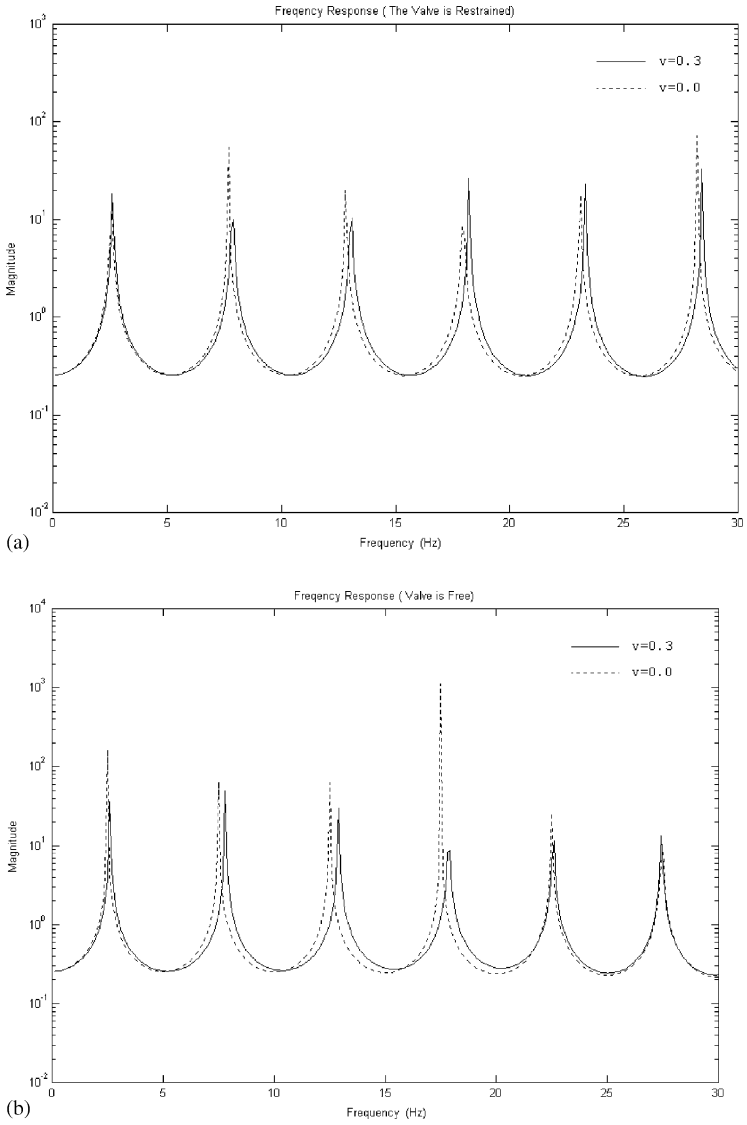

Fig. 7. Frequency responses of the RPV system with 5 spans (20 m length for each span). (a) Valve is rigid constrained, (b) valve is free.

shown in Fig. 9(b) we believe that it is indeed the mode shape of the pipe, since its frequency is near the first frequency of a solid bar with 20 m (128.9 Hz).

5. Conclusion

Vibration analysis considering fluid–structure interaction in liquid-filled pipe systems is performed in frequency domain using the transfer matrix method (TMM). It extends the

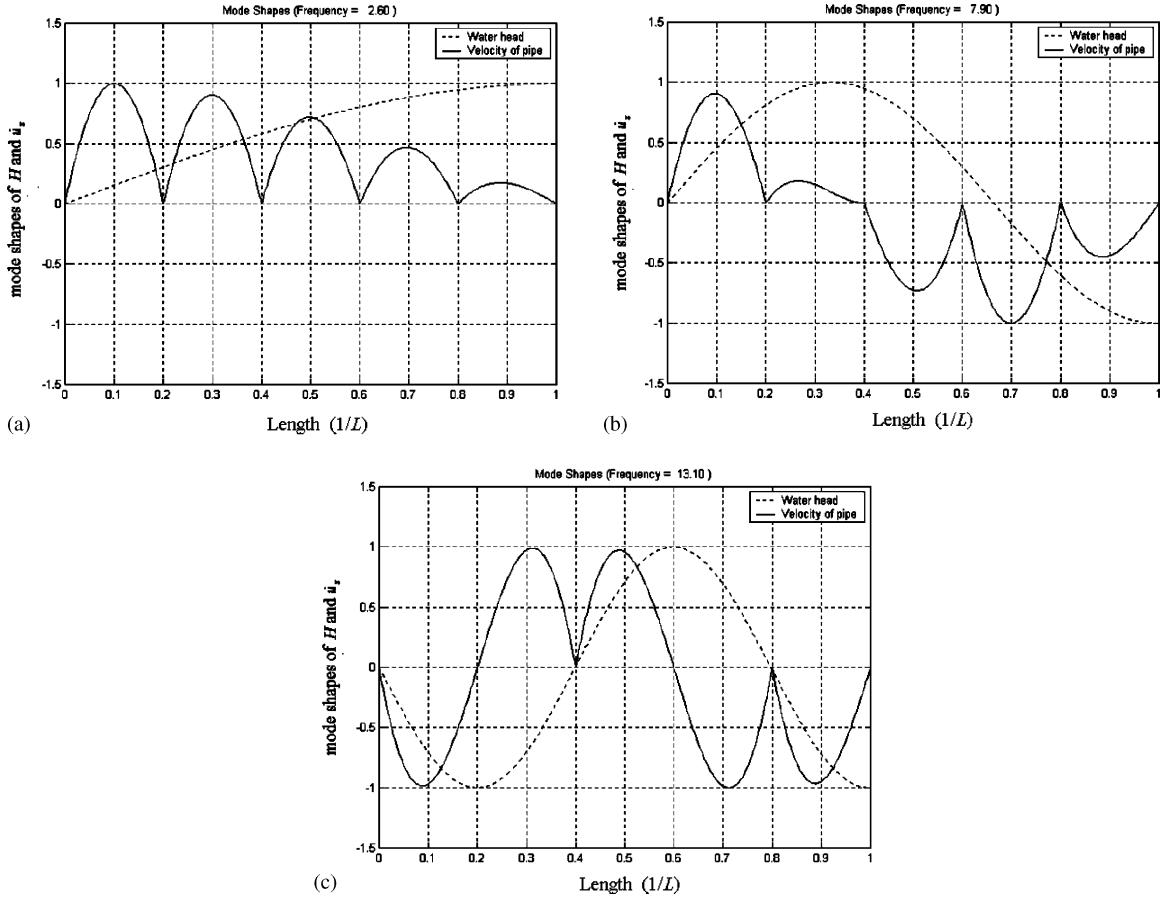

Fig. 8. Modes 1–3 of the pipe system with 5 spans.

frequency domain based vibration analysis considering FSI presented in Ref. [26] from single-span pipe to multi-span pipeline systems with rigid constraints. The emphasis is placing especially upon the vibration analysis of multi-span pipeline systems with middle rigid constraints, since such a problem is always encountered in engineering practices.

In order to solve the title problem by using TMM, 4 variables should be transferred from one span to another. The TMM proposed in this paper solve this problem by combining the pipe variables into the transfer equations. A special phenomenon associated with rigid constraints has been identified, and the conditional junction coupling is revealed and studied. It is found that the conditional junction coupling is a junction coupling depending on the Poisson coupling and friction coupling. Therefore, the three major coupling mechanisms are actually not totally independent. The numerical examples indicate that the conditional junction coupling has much larger influence on the frequencies of a pipe system than the Poisson coupling does. It is also shown through the numerical examples that the proposed method is efficient.

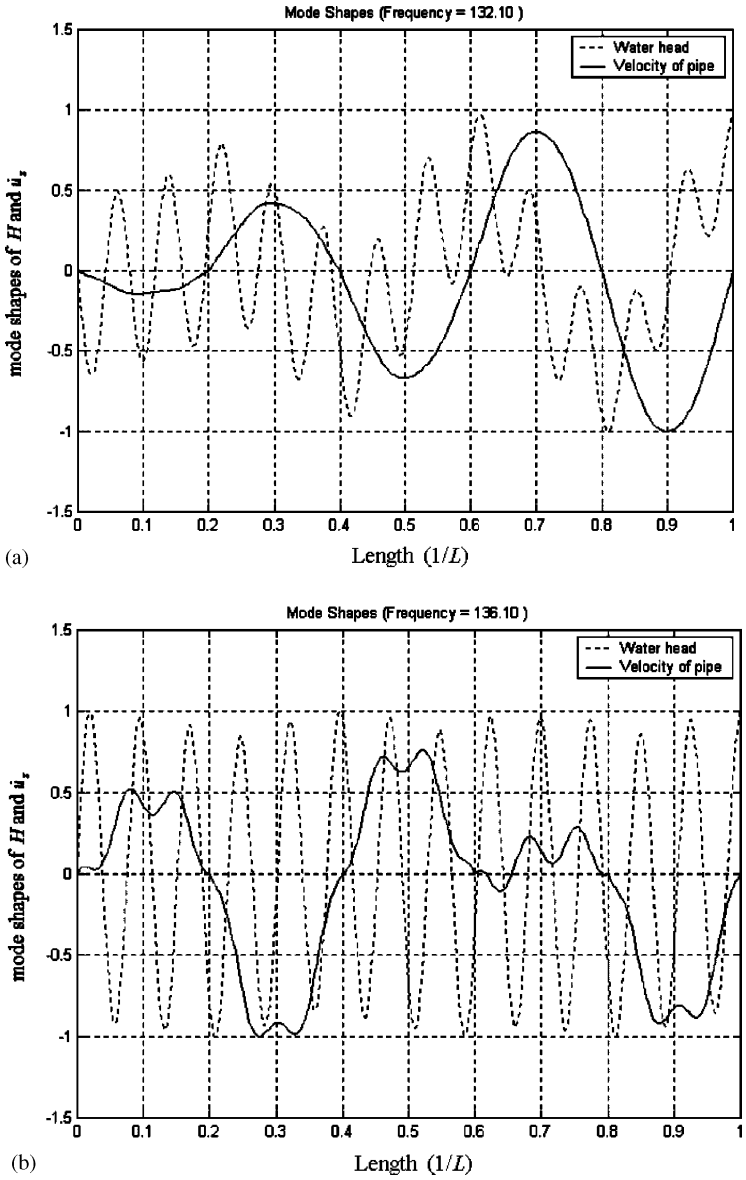

Fig. 9. The 1st pipe mode shape and nearby fluid mode shape of the pipe system with 5 spans and constrained valve. (a) Frequency = 132.1 Hz, (b) frequency = 136.1 Hz.

The proposed TMM considers the three major mechanisms of coupling and can deal with vibration analysis of a multi-span pipe system with different geometry and material properties and subjected to both distributed and concentrated external excitations. Furthermore, with the proposed TMM, the transient response in time domain would be possibly determined by taking inverse Laplace transforms.

Acknowledgements

The authors are thankful to the reviewers for their valuable comments and suggestions. The financial supports provided by the National Natural Science Foundation of China (Project No.50079007) and The Ministry of Water Resources, China (Project No. SZ9830) for the study described in this paper are gratefully acknowledged.

References

[1] M.P. Paidoussis, *Fluid-Structure Interactions*, San Diego Academic Press, London, 1998.
[2] A.S. Tijsseling, Fluid–structure interaction in liquid-filled pipe systems: a review, *Journal of Fluids and Structures* 10 (1996) 109–146.
[3] L.X. Zhang, W.H. Huang, Fluid–structure interaction in least constrained piping systems: a review, *Journal of Hydrodynamics A* 14 (1) (1999) 102–111.
[4] E.B. Wylie, V.L. Streeter, *Fluid Transients in Systems*, Prentice Hall, Englewood Cliffs, NJ, 1993.
[5] A.R.D. Thorley, Pressure transients in hydraulic pipelines, *American Society of Mechanical Engineers Journal of Basic Engineering* 91 (1969) 453–461.
[6] A.E. Vardy, D. Fan, Water Hammer in A Closed Tube, *Proceedings of the 5th International Conference on the Pressure Surge*, BHRA, Hanover, Germany, Sept., 1986, pp. 123–137.
[7] A.F. D'souza, R. Oldenburger, Dynamic response of fluid lines, *American Society of Mechanical Engineers, Journal of Basic Engineering* 86 (1964) 589–598.
[8] J. Charley, G. Caignaert, Vibroacoustical analysis of flow in pipes by transfer matrix with fluid–structure interaction, *Proceedings of the 6th International Meeting of the IAHR Work Group on the Behavior of Hydraulic Machinery under Steady Oscillatory Conditions*, Lausanne, Switzerland, September 1993, pp. 1–9.
[9] J. Charley, F. Carta, Application of the auto- and cross-power spectra to hydro-and aeroacoustics, *Mechanical Systems and Signal Processing* 15 (2) (2000) 399–417.
[10] D.H. Wilkinson, Acoustic and mechanical vibrations in liquid-filled pipework systems, *Proceedings of the BNES International Conference on Vibration in Nuclear Plant*, Paper 8.5, Keswick, UK, May, 1978, pp. 863–878.
[11] M. EL-Raheb, Vibrations of three-dimensional pipe systems with acoustic coupling, *Journal of Sound and Vibration* 78 (1981) 39–67.
[12] S. Nanayakkara, N.D. Perreira, Wave propagation and attenuation in piping systems, *American Society of Mechanical Engineers, Journal of Vibration, Acoustics, Stress, and Reliability in Design* 108 (1986) 441–446.
[13] G.D.C. Kuiken, Amplification of pressure fluctuations due to fluid–structure interaction, *Journal of Fluids and Structures* 2 (1988) 425–435.
[14] M.W. Lesmez, Modal Analysis of Vibrations in Liquid-filled Piping Systems, Ph.D.Thesis, Department of Civil and Environmental Engineering, Michigan State University, East Lansing, USA, 1989.
[15] M.W. Lesmez, D.C. Wiggert, F.J. Hatfield, Modal analysis of vibrations in liquid-filled piping systems, *American Society of Mechanical Engineers, Journal of Fluids Engineering* 112 (1990) 311–318.
[16] F.J. Hatfield, D.C. Wigger, R.S. Otwell, Fluid structure interaction in piping by component method, *American Society of Mechanical Engineers, Journal of Fluid Engineering* 104 (1982) 318–325.
[17] D.C. Wiggert, F.J. Hatfield, S. Stuckenbruck, Analysis of liquid and structural transients by the method of characteristics, *American Society of Mechanical Engineers, Journal of Fluids Engineering* 109 (2) (1987) 161–165.
[18] S.C. Tentarelli, F.T. Brown, Dynamic behavior of complex fluid-filled systems—Part II: System Analysis, *American Society of Mechanical Engineers, Journal of Dynamic Systems, Measurement and Control* 123 (1) (2001) 78–84.
[19] F.T. Brown, S.C. Tentarelli, Dynamic behavior of complex fluid-filled systems—Part I: Tubing Analysis, *American Society of Mechanical Engineers, Journal of Dynamic Systems, Measurement and Control* 123 (1) (2001) 71–77.
[20] C.A.F. De Jong, Analysis of Pulsation and Vibrations in Fluid-filled Pipe Systems, Ph.D. Thesis, Eindhoven University of Technology, Eindhoven, The Netherlands, ISBN 90-386-0074-7, 1994.

[21] C.A.F. De Jong, Analysis of pulsation and vibrations in fluid-filled pipe systems, *Proceedings of the 1995 Design Engineering Technical Conferences*, Part B, ISBN 0-7918-1718-0, pp. 829-834, Boston, USA, September, 3, 1995.
[22] J.-S. Wu, P.-Y. Shih, The dynamic analysis of a multispan fluid-conveying pipe subjected to external load, *Journal of Sound and Vibration* 239 (2) (2001) 201–215.
[23] L.X. Zhang, W.H. Huang, Frequency response analysis in internal flows, *Journal of Hydro-dynamics Series B* 3 (1995) 39–49.
[24] L.X. Zhang, A.S. Tijsseling, A.E. Vardy, FSI frequency response analysis of flexible pipes, *Journal of Chinese Engineering Mechanics* 13 (2) (1996) 69–77.
[25] L.X. Zhang, Frequency response analysis of pipeline under any excitation, *Journal of Hydrodynamics B* 4 (1998) 71–89.
[26] L.X. Zhang, A.S. Tijsseling, A.E. Vardy, FSI analysis of liquid-filled pipes, *Journal of Sound and Vibration* 224 (1) (1999) 66–99.
[27] K. Yang, Fluid–Structure Interaction in Liquid-filled Piping System and Reliability of Time-dependent Structures, Ph.D. Dissertation, Wuhan University of Technology, 1999.
[28] A.S. Tijsseling, Fluid–Structure Interaction in Case of Water-Hammer with Cavitation, Ph.D Thesis, Delft University of Technology, 1993.